

Binding energies and diamagnetic shifts for free excitons in symmetric coupled double quantum wells

Q. X. Zhao, B. Monemar, P. O. Holtz, and M. Willander

Department of Physics and Measurement Technology, Linköping University, S-581 83 Linköping, Sweden

B. O. Fimland

Department of Physical Electronics, Norwegian Institute of Technology, N-7034 Trondheim, Norway

K. Johannessen

SINTEF DELAB, N-7034 Trondheim, Norway

(Received 8 March 1994)

A simple method for calculating the free-exciton binding energies in the fractional-dimensional-space model for single-quantum-well (SQW) structures has been extended to symmetric coupled double quantum wells (CDQW). We also apply these results to estimate the diamagnetic shift of the free excitons for both CDQW and SQW systems. Corresponding experimental photoluminescence data are obtained on CDQW and SQW samples grown by molecular-beam epitaxy. The calculated binding energies and diamagnetic shifts show good agreement with the experimental data.

I. INTRODUCTION

When the thickness of a barrier layer which separates two quantum wells (QW's) is sufficiently small, the two wells become electronically coupled. Such structures, coupled double quantum wells (CDQW's), are interesting because they have electronic and optical properties which can be utilized in optoelectronic devices. An important method to investigate such CDQW structures is optical characterization, such as photoluminescence (PL) and PL excitation measurements with different perturbations (such as magnetic field, mechanical stress, and electric field). The PL spectra of the CDQW structures are usually dominated by the excitons. The effects of electric fields on excitons in undoped GaAs/Al_xGa_{1-x}As CDQW structures have been studied by Chen *et al.*,¹ who show a detailed experimental investigation of the quantum-confined Stark effect, intrawell and interwell exciton transitions. The influence of electric fields on exciton lifetimes in GaAs/Al_xGa_{1-x}As CDQW structures was also reported later.² However, there is very little experimental work reported concerning the exciton binding energies in CDQW structures,³ and there is, to our knowledge, no theoretical or experimental work reported concerning the diamagnetic shift of the excitons in such structures.

Theoretical calculations of the exciton binding energy have been reported by several authors⁴⁻⁶ for CDQW structures. The calculations were based on variational methods. The accuracy of the results is then very dependent on the choice of the trial wave function. Besides, the excited states of the excitons are not dealt with in most of the previous work. Such variational calculations for CDQW structures are very demanding on computer time in comparison with single QW structures.

Recently, a simple analytical method has been developed by Mathieu, Lefebvre, and Christol⁷ (in the fol-

lowing denoted as the MLC method) to calculate the exciton binding energies in single QW (SQW) structures. The method uses the model of fractional-dimensional space. The spatial dimension α , which measures the anisotropy of the electron-hole interaction, changes continuously from 3 to 2 (or 1) for ideal three-dimensional (3D) to 2D (or 1D) systems, respectively.⁷ The results obtained by this technique are surprisingly accurate in comparison with very advanced calculations in single QW systems.⁸

In this paper, we have extended the MLC method to study CDQW structures. The calculated exciton binding energies are compared with our recent experimental results at zero magnetic field.³ The diamagnetic shifts of excitons are also measured and calculated in this work (up to 6 T) for the CDQW and the single QW structures. In Sec. II the samples and experimental techniques are described. The experimental results on the diamagnetic shifts are presented in Sec. III. In Sec. IV the main analytic expressions from the MLC method are simply recalled. This is important to make the discussion of the extension of the MLC formalism clearer in the following section. In Sec. V the extension of the MLC to CDQW structures is presented from this theoretical approach. The results are compared with the experimental data in Sec. VI. Finally, a summary is given.

II. SAMPLES AND EXPERIMENTAL SETUP

The samples were grown in a Varian Gen II modular molecular-beam epitaxy machine on [001]-oriented semi-insulating GaAs substrates. The growth was started with a 5000-Å-thick GaAs buffer layer, followed by a 20-period superlattice consisting of 20-Å AlAs and 20-Å GaAs layers. After the superlattice buffer layer, an 800-Å Al_{0.3}Ga_{0.7}As barrier was grown. On top of this barrier

double QW structures with equal $\text{Al}_{0.3}\text{Ga}_{0.7}\text{As}$ barrier thickness L_b and decreasing QW widths (L_z) were grown. The double wells were separated by 800-Å $\text{Al}_{0.3}\text{Ga}_{0.7}\text{As}$ barrier layers. The growth was ended with an 800-Å-thick $\text{Al}_{0.3}\text{Ga}_{0.7}\text{As}$ barrier layer and a 200-Å-thick GaAs capping layer. The Be impurities are in the center of the wells, with a doping concentration of $1 \times 10^{17} \text{ cm}^{-3}$. The two doped symmetric CDQW's (SCDQW's) with nominal well widths of $L_z = 150.0$ and 99.1 Å and the four undoped SCDQW's with well widths of $L_z = 150.0$ and 99.1 Å, and $L_z = 124.5$ and 79.2 Å are studied. All double wells have a nominal barrier thickness $L_b = 14.2$ Å. Two doped SQW's with nominal well widths 99.1 and 150.0 Å, grown in a similar way as the SCDQW, were used as reference samples in this study.

The photoluminescence measurements were done in a 16-T superconducting magnet. The laser was coupled to the samples via optical fibers, and the PL emissions from the samples were collected through the same fiber into the monochromator. The excitation source was an Ar^+ laser (5145 Å). A GaAs photomultiplier was used to detect the PL signals. The data presented are measured in the Faraday configuration.

III. EXPERIMENTAL RESULTS

PL spectra at different magnetic fields are measured both for the SCDQW and the SQW structures. The diamagnetic shifts of the free excitons (FE's) in the doped SCDQW's are the same as in the undoped SCDQW's. Figure 1 shows PL spectra for the SCDQW with doped 99-Å-wide wells at four different magnetic fields. Two dominating transitions, the symmetric heavy hole (hh) FE and acceptor bound excitons (BE), appear in the PL spectra at flat-band conditions. Detailed optical studies

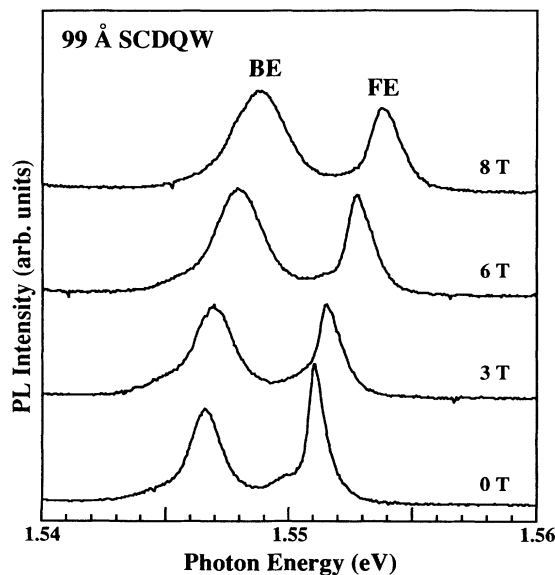


FIG. 1. PL spectra from a 99-Å-wide CDQW sample with a 14.2-Å barrier layer, measured at 2.0 K at different magnetic fields under flat-band conditions.

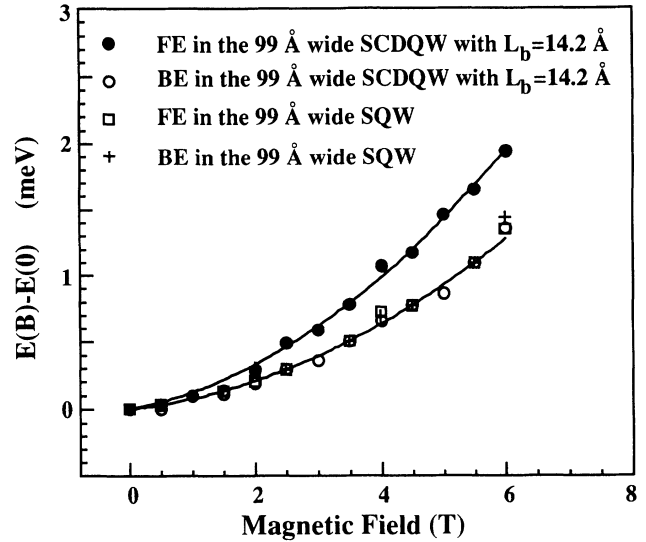


FIG. 2. The magnetic-field dependence of the FE and the BE peak energies for the 99-Å-wide SCDQW and the 99-Å-wide SQW structures. The solid lines are fitted to experimental data to deduce the diamagnetic shift.

of the hh FE and the BE with an applied electric field on these samples have been reported previously.^{9,10} It was shown that both the interwell and intrawell FE and BE can be observed with an electric field across the SCDQW structures, and the binding energies of the interwell and the intrawell BE are equal. PL spectra from different samples are measured up to 6 T; the diamagnetic shifts of the excitons are deduced by fitting the data. In Fig. 2 the energy shifts of the excitons with magnetic field relative to energy position of the excitons at zero field are shown for a 99-Å-wide SCDQW and for a reference 99-Å-wide SQW, respectively, at flat-band conditions. For the SQW, the energy shifts are similar for the FE and the BE, and also for the BE in the SCDQW. This is consistent with the conclusion from the previous work that the BE is not significantly influenced by the coupling between the two wells for a 99-Å-wide SCDQW structure with a 14.2-Å-wide barrier,⁹ while the FE exhibits a larger diamagnetic shift for the SCDQW than for the corresponding SQW. The diamagnetic shifts have been deduced by fitting the data in a least-squares-fitting procedure,¹¹ and are summarized in Table I. In Table II, the $1S$ - $2S$ energy separations of the symmetric hh FE from previous studies³ are also included. These results will be further compared with theoretical calculations later in this paper.

TABLE I. The diamagnetic shifts of the hh FE for the GaAs/ $\text{Al}_{0.3}\text{Ga}_{0.7}\text{As}$ SCDQW and the GaAs/ $\text{Al}_{0.3}\text{Ga}_{0.7}\text{As}$ SQW structures.

L_z (Å)	CDQW hh FE (meV/T ²)	Single QW hh FE (meV/T ²)
79.2	0.035	
99.1	0.040	0.027
124.5	0.045	
150.0	0.051	0.038

TABLE II. The 1S-2S energy separations of the hh FE for the GaAs/Al_{0.3}Ga_{0.7}As SCDQW structures.

L_z (Å)	L_b (Å) ($x=0.3$)	1S-2S (meV) hh excitons
99.1	14.2	5.65
79.2	14.2	6.50
59.4	14.2	7.79
79.2	19.8	6.75
59.4	19.8	7.98

IV. THE ANALYTIC MLC EXPRESSIONS FOR EXCITONS IN SINGLE QW'S

By using the fractional-dimensional model proposed by He,¹² the exciton problem in QW structures can be treated as one of a hydrogenlike atom. In the fractional-dimensional model adopted, the Schrödinger equation is solved in a noninteger-dimensional space where the interactions are assumed to occur in an isotropic environment. The discrete excitonic bound-state energies and orbital radii are then given by

$$E_n = E_g - \frac{E_0}{\left[n + \frac{\alpha-3}{2} \right]^2}, \quad (1)$$

$$a_n = a_0 \left[n + \frac{\alpha-3}{2} \right]^2,$$

where $n = 1, 2, \dots$, is the principal quantum number, E_0 and a_0 are the effective Rydberg constant and effective Bohr radius, respectively, expressed in terms of the Rydberg constant R_H and the Bohr radius a_H ,

$$E_0 = \left[\frac{\epsilon_0}{\epsilon} \right]^2 \left[\frac{\mu}{m_0} \right] R_H, \quad (2)$$

$$a_0 = \left[\frac{\epsilon}{\epsilon_0} \right] \left[\frac{m_0}{\mu} \right] a_H,$$

m_0 is the free-electron mass and μ is the exciton reduced mass, $1/\mu = 1/m_e + 1/m_h$. According to Eq. (1), the binding energy of the 1S exciton is given by

$$E_b = \left[\frac{2}{\alpha-1} \right]^2 E_0. \quad (3)$$

α corresponds to the dimensionality and the related exciton binding energy is given by $E_b = E_0, 4E_0$, or ∞ for $\alpha = 3, 2$, or 1, respectively, corresponding to the well-known results of the integer-dimensional models. Thus, the main problem is to define the fractional dimension α , which describes the degree of anisotropy of the electron-hole interaction. For the SQW structures, MLC have demonstrated⁷ that the dimensionless parameter α is given by

$$\alpha = 3 - e^{-L_w^*/2a_0^*}, \quad (4)$$

$$L_w^* = \frac{2}{k_b} + L_w, \quad (5)$$

$$\frac{1}{k_b} = \frac{1}{k_{be}} + \frac{1}{k_{bh}},$$

$$a_0^* = \frac{\epsilon m_0}{\epsilon_0 \mu^*} a_H. \quad (6)$$

Here k_{be} and k_{bh} are the electron and hole eigen-wavevectors of the Schrödinger equation in the barrier material region of the QW. L_w is the well width of the QW and μ^* is the mean value of the 3D reduced mass of the exciton, which is given by $1/\mu^* = 1/m_e^* + 1/m_h^*$.

Concerning the effective-mass mismatch between the well and the barrier materials, MLC have defined the two weighting parameters β_e and β_h as

$$\beta_e = \frac{L_w}{\left[\frac{2}{k_{be}} + L_w \right]}, \quad (7)$$

$$\beta_h = \frac{L_w}{\left[\frac{2}{k_{bh}} + L_w \right]}.$$

Then the mean values for the electron effective mass and valence-band Luttinger parameters are given by

$$m_e^* = m_{ew} + (1 - \beta_e) m_{eb},$$

$$\gamma_1^* = \beta_h \gamma_{1w} + (1 - \beta_h) \gamma_{1b}, \quad (8)$$

$$\gamma_2^* = \beta_h \gamma_{2w} + (1 - \beta_h) \gamma_{2b}.$$

Furthermore, MLC have taken into account the conduction-band nonparabolicity and dielectric-constant mismatch effects by introducing the following mean values of electron effective mass and mean dielectric constant:

$$m_{ew} = m_{ew0} [1 + (2\alpha' + \beta') E_p], \quad (9a)$$

$$m_{eb} = m_{eb0} [1 + (2\alpha' + \beta') (V_e - E_p)], \quad (9b)$$

where m_{ew0} and m_{eb0} are the band-edge effective masses in the well and the barrier materials, respectively. V_e is the electron-quantum-well depth, E_p is the confinement energy. For GaAs, $\alpha' = 0.64 \text{ eV}^{-1}$ and $\beta' = 0.70 \text{ eV}^{-1}$, and the same values are used for the barrier material. The mean dielectric constant is given by

$$\epsilon^* = \sqrt{\beta_e \beta_h} \epsilon_w + (1 - \sqrt{\beta_e \beta_h}) \epsilon_b. \quad (10)$$

By using Eq. (1) together with Eq. (4), a very simple expression to obtain the binding energy of the confined exciton in a finite quantum well is given by MLC,

$$E_{nb} = \frac{E_0^*}{\left[n - \frac{1}{2} e^{-L_b^*/2a_0^*} \right]^2}, \quad (11)$$

where E_0^* is the mean value of the effective Rydberg energy for the three-dimensional exciton, which is calculated using the following expressions for the reduced masses:

$$\begin{aligned} \frac{1}{\mu_{hh}^*} &= \frac{1}{m_e^*} + \gamma_1^* + (3-\alpha)\gamma_2^* , \\ \frac{1}{\mu_{lh}^*} &= \frac{1}{m_e^*} + \gamma_1^* - (3-\alpha)\gamma_2^* . \end{aligned} \quad (12)$$

So far we have just briefly reviewed the MLC formalism leading to the analytical expressions for exciton binding energies in single QW's. It has been demonstrated that these simple calculations for confined exciton binding energy are reasonably good for SQW's.⁷

V. EXTENSION OF THE MLC FORMALISM TO COUPLED DOUBLE QUANTUM WELLS

In this section, we extend the MLC model to calculate the exciton binding energies in the CDQW. Proper computer calculations of the exciton binding energy in a CDQW system are considerably more time consuming than for the SQW system, since more excited states need to be included in a CDQW system. Therefore, it is very helpful to deduce a simple formula to calculate the exciton binding energies in a CDQW. Figure 3 shows the schematic potential for a CDQW structure. L_{1w} and L_{2w} are the two coupled well widths, L_b is the barrier thickness separating the two wells. The eigen-wave-functions ψ_n^i and eigenenergies E_n^i are solutions of the following Schrödinger equation:

$$H_i \psi_n^i = E_n^i \psi_n^i , \quad (13)$$

$$H_i = -\frac{\hbar^2}{2} \frac{\partial}{\partial z} \frac{1}{m_i} \frac{\partial}{\partial z} + V_i(z) . \quad (14)$$

Here the z axis is the growth axis of the structures. $V_i(z)$ are the potential of the CDQW, with $i \in \{e, hh, lh\}$. The wave vectors and confined energies have the following relation:

$$\begin{aligned} E_n &= \frac{\hbar^2 k_w^2}{2m_w} , \\ V_0 - E_n &= \frac{\hbar^2 k_b^2}{2m_b} . \end{aligned} \quad (15)$$

Here m_w and m_b are the effective masses in the wells and the barriers, respectively. V_0 is the band offset between the well and the barrier materials.

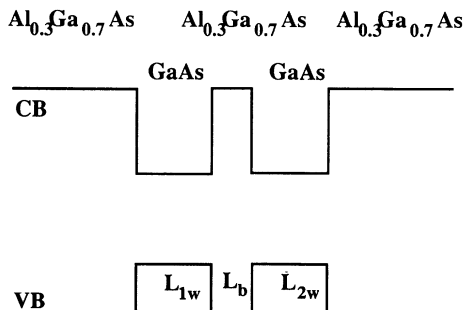


FIG. 3. The schematic potential for the CDQW structures.

When extending the MLC model to calculate such CDQW structures, an important aspect is how to define the dimensionless parameter α . If we consider the two coupled wells as an effective SQW with an effective well width $L_{\text{eff},w}$, the analytical formula (4) may be directly applicable here to calculate the parameter α , by simply replacing the SQW width L_w with the effective well width $L_{\text{eff},w}$. Now let us look at two limiting cases for a CDQW structure: When the barrier thickness $L_b=0$, the coupled QW becomes a SQW with the well width $L_{\text{eff},w}=L_{1w}+L_{2w}$. When L_b is going to infinity on the other hand, the coupled QW's become two independent SQW's with well widths L_{1w} and L_{2w} , respectively, i.e., $L_{\text{eff},w}=L_{1w}$ or $L_{\text{eff},w}=L_{2w}$.

From now on all our discussions are based on the choice of the L_{1w} well as the main well and the L_{2w} well as the perturbation well, assuming that $L_{1w} \geq L_{2w}$. The opposite case can easily be obtained by interchange of the two well widths.

Based on the above two limiting cases, $L_{\text{eff},w}$ may be written as

$$L_{\text{eff},w} = L_{1w} + L_{2w} e^{-L_b k} . \quad (16)$$

Here the parameter k characterizes the interaction between the two wells. Since the interaction between the two wells is dependent on the overlap of the respective wave functions, and concern both the electron and the hole involved in the excitons, the parameter k may be given by

$$\frac{1}{k} = \frac{1}{k_{be}} + \frac{1}{k_{bh}} . \quad (17)$$

Here k_{be} and k_{bh} , which are solutions of the Schrödinger equation (13) of the electron and the hole in the CDQW system, are defined by Eq. (15) for the electron and the hole in the barrier layer, respectively. By using Eqs. (4) and (7)–(17), the binding energies of the S -like exciton states can be calculated for the CDQW structures. The measured hh FE 1S-2S energy-separation for the excitons can be compared with the energy separation $E_{1b}-E_{2b}$ calculated from expression (11) (see Fig. 5). The effective Bohr radius of the excitons can also be estimated as

$$a_n = \left[\frac{\epsilon_0}{\epsilon} \right] \left[\frac{m_0}{\mu^*} \right] a_H \left[n + \frac{\alpha-3}{2} \right]^2 . \quad (18)$$

μ^* is the effective mass of the excitons. The diamagnetic shift of the excitons (ΔE) is directly correlated with the effective Bohr radius and the effective mass of the exciton. Accordingly, ΔE can be estimated by¹³

$$\Delta E = (eB)^2 \left[\frac{a_n^2}{2\mu^*} \right] \alpha_2 . \quad (19)$$

Here B is the applied magnetic field, and α_2 is a constant. In the Faraday configuration (σ components) $\alpha_2=0.462$ in bulk GaAs.¹³ In the derivation of this expression, no additional important assumption was made except for the spherical symmetry of the binding Coulomb potential. For excitons in a 2D system we may expect some difference of the constant α_2 due to a lower symmetry.

TABLE III. The parameters used in the calculations.

	GaAs	$\text{Al}_x\text{Ga}_{1-x}\text{As}$
m_{e0}	$0.0667m_0$	$(0.0667+0.083x)m_0$
m_{hh0}	$0.34m_0$	$(0.34+0.42x)m_0$
m_{lh0}	$0.094m_0$	$(0.094+0.043x)m_0$
ϵ_r	12.5	$12.5(1-x)+9.8x$

The parameters used in our calculations are listed in Table III. The band offset between the conduction and valence band is taken as 0.65:0.35, and the band-gap energy difference between GaAs and $\text{Al}_x\text{Ga}_{1-x}\text{As}$ is $\Delta E = 1.455x$.

VI. COMPARISON BETWEEN CALCULATED AND EXPERIMENTAL DATA

By using Eqs. (4) and (7)–(17), the binding energies of the symmetric hh FE in SCDQW structures (i.e., $L_{1w} = L_{2w}$) versus the well widths are calculated. Figure 4 shows the results with different barrier widths between the two wells as a parameter. The hh FE binding energies are reduced with decreasing barrier width, and the well width corresponding to the maximum binding energy is shifted towards narrower wells with decreasing barrier thickness. These results reflect the effects of increasing the effective well width with decreasing the barrier thickness. Figure 5 shows the calculated 1S-2S energy separations of the symmetric hh FE at two different barrier widths in the SCDQW structures. Our experimental data of the 1S-2S energy separation of the hh FE are also shown for comparison.³ The reduction of the hh FE binding energy for the SCDQW structures, in comparison with the corresponding SQW structures (see Fig. 4), is consistent with an increase of the FE diamagnetic shift.

The diamagnetic shifts are calculated according to Eqs.

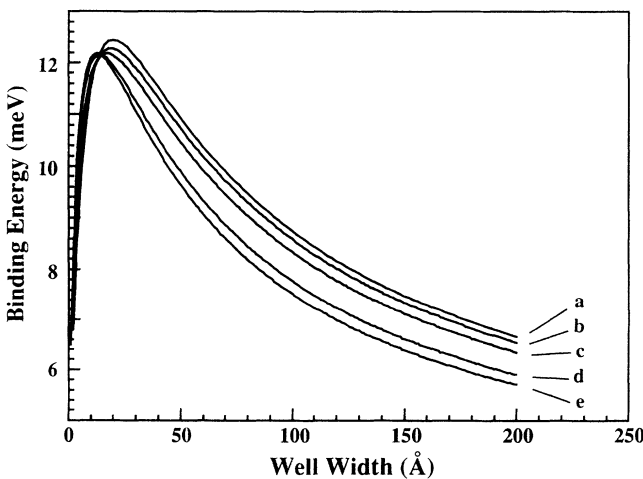


FIG. 4. The FE binding energies calculated according to the text for a, GaAs/ $\text{Al}_{0.3}\text{Ga}_{0.7}\text{As}$ SQW, and for the GaAs/ $\text{Al}_{0.3}\text{Ga}_{0.7}\text{As}$ CDQW with b, 60-Å-, c, 40-Å-, d, 20-Å-, and e, 14.2-Å-wide barrier.

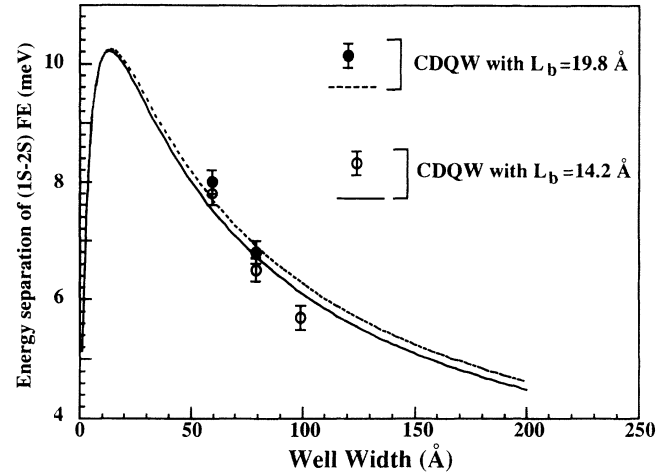


FIG. 5. The dependence of the 1S-2S energy separation of the hh FE on L_z . The solid and dashed lines show the corresponding calculated dependence according to $E_{1b} - E_{2b}$ by using Eq. (11). The points are experimental results for two SCDQW's.

(18) and (19) for the 1S hh FE in both the SCDQW and the SQW structures, i.e., $n = 1$ in Eq. (18). The solid lines in Fig. 6 show the calculated diamagnetic shifts for the single QW versus well widths with different values of the constant α_2 . The experimental results (the solid circles) are also indicated in the figure for comparison. Figure 7 shows the calculated exciton diamagnetic shifts for the CDQW structures with the barrier width $L_b = 14.2$ Å at different values of the constant α_2 . The data from the SQW and the SCDQW indicate that α_2 is close to 0.4 in the QW structures. The agreement is very good within the experimental accuracy if we use the constant $\alpha_2 = 0.4$ for both the SQW and the SCDQW. The deduced value of 0.4 is accordingly very close to the bulk GaAs value of 0.462.

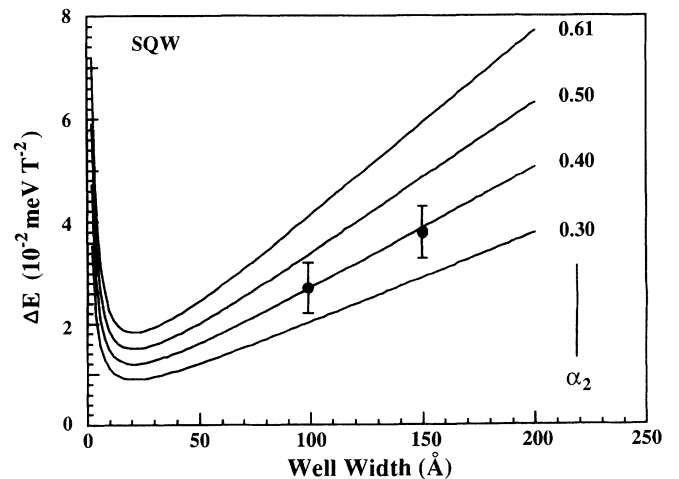


FIG. 6. The FE diamagnetic shifts vs well size for single QW structures calculated according to Eq. (19) at different values of the α_2 constant. The points correspond to experimental results.

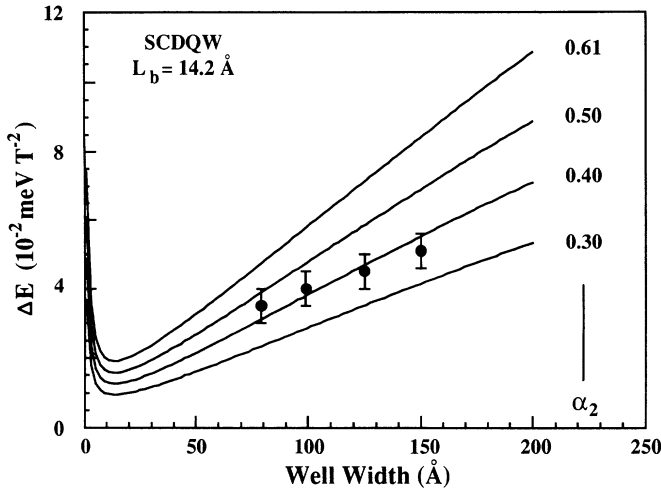


FIG. 7. The FE diamagnetic shifts vs well width for the SCDQW structures with 14.2-Å barrier width calculated according to Eq. (19) at different values of the α_2 constant. The points correspond to experimental results derived for structures with various QW widths.

We would like to point out that the calculations for the exciton binding energy in the CDQW structures discussed above only partly take into account the effect of the dielectric-constant mismatch by the averaging procedure of Eq. (10). The electrostatic effect of image charges is neglected, which is even more complicated in CDQW structures than in single QW's. Nevertheless,

such image charge effects due to dielectric-constant mismatch in single QW's have been estimated in Ref. 7 by using a simple analytical expression [Eq. (28) in Ref. 7],

$$\Delta E_B = 2(\epsilon_w - \epsilon_b) / (\epsilon_w + \epsilon_b) \frac{e^2}{\epsilon_w L_w} \times [1 - \exp(-1.7L_w/a_0^*)]. \quad (20)$$

In a first approximation, we can also use the same expression for CDQW structures, by simply replacing the well width L_w of a single QW in Eq. (20) to the effective well width $L_{\text{eff.w}}$ in CDQW structures. The resulting change of the exciton binding energy varies from 0.30 to 0.65 meV for the CDQW with a constant 14.2-Å barrier when the well width is reduced from 150 to 50 Å, respectively.

VII. SUMMARY

A simple analytical model for isolated QW's has been extended to calculate the exciton binding energies of CDQW structures. The calculations are compared with our recent experimental results. The diamagnetic shifts of the excitons, both for the single and symmetric coupled double QW structures, are calculated and compared with our experimental results. The calculated and experimental results show good agreement both for exciton binding energies and the exciton diamagnetic shifts in the CDQW structures. By using the simple hydrogenic model, the diamagnetic shift data for both the single QW and the CDQW structures indicate that the constant α_2 is close to 0.4.

- ¹Y. J. Chen, Emil S. Koteles, B. S. Elman, and C. A. Armiento, Phys. Rev. B **36**, 4562 (1987).
²S. Charbonneau, M. L. W. Thewalt, Emil S. Koteles, and B. Elman, Phys. Rev. B **38**, 6287 (1988).
³Q. X. Zhao, B. Monemar, T. Westgaard, B. O. Fimland, and K. Johannessen, Phys. Rev. B **46**, 12 853 (1992).
⁴T. Kamizato and M. Matsuura, Phys. Rev. B **40**, 8378 (1989).
⁵M. M. Dignam and J. E. Sipe, Phys. Rev. B **43**, 4084 (1991).
⁶T. Westgaard, Q. X. Zhao, B. O. Fimland, K. Johannessen, and L. Johnsen, Phys. Rev. B **45**, 1784 (1992).
⁷H. Mathieu, P. Lefebvre, and P. Christol, Phys. Rev. B **46**, 4092 (1992).
⁸L. C. Andreani and A. Pasquarello, Phys. Rev. B **42**, 8928

(1990).

- ⁹Q. X. Zhao, T. Westgaard, B. O. Fimland, and K. Johannessen, Phys. Rev. B **45**, 11 346 (1992).
¹⁰Q. X. Zhao, T. Westgaard, B. Monemar, B. O. Fimland, and K. Johannessen, Proceedings of the Fifth International Conference on Shallow Impurities in Semiconductors, edited by T. Taguchi [Materials Science Forum **117&118**, 333 (1993)].
¹¹Q. X. Zhao and T. Westgaard, Phys. Rev. B **44**, 3726 (1991).
¹²X. F. He, Phys. Rev. B **43**, 2063 (1991).
¹³M. Altarelli and Nunzio O. Lipari, Phys. Rev. B **7**, 3798 (1973).